JOC The Journal of Organic Chemistry

Article

pubs.acs.org/joc

When To Let Go—Diradical Intermediates from Zwitterionic Transition State Structures?

Q. Nhu N. Nguyen and Dean J. Tantillo*

Department of Chemistry, University of California—Davis, Davis, California 95616, United States

Supporting Information

ABSTRACT: Several Brummond–Chen thermal intramolecular (2 + 2)-cycloaddition reactions were examined using density functional theory calculations. The results of these calculations indicate that it is possible for these reactions to involve diradical intermediates that form directly from zwitterionic transition state structures. The likelihood of this scenario was shown to be sensitive to both the nature of substituents and solvent polarity.

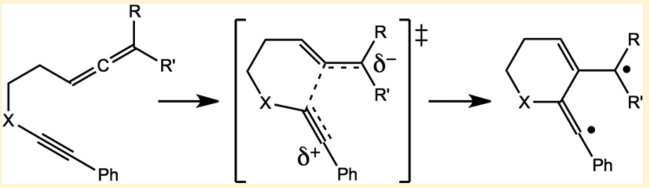

INTRODUCTION

Thermal reactions that produce organic diradicals from closed-shell precursors have been of interest to both mechanistic and synthetic chemists for decades. For example, the Bergman cyclization, first reported in the early 1970s, introduced a means of generating *para*-benzyne diradicals from ene-diyenes (Scheme 1a).[1] In the late 1980s, related reactions (Myers–Saito reactions) were discovered in which aryl/benzyl diradicals could be generated from conjugated allene-ene-ynes (Scheme 1b).[2] Both of these types of reaction were found to play a role in the mechanism of action of natural products with antibiotic activity.[3] Schmittel and co-workers described the thermal generation of different diradical intermediates from conjugated allene-ene-ynes

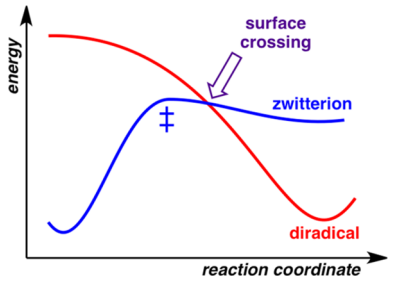

Figure 1. Qualitative picture of a post-transition state surface crossing (e.g., conical intersection).

Scheme 1

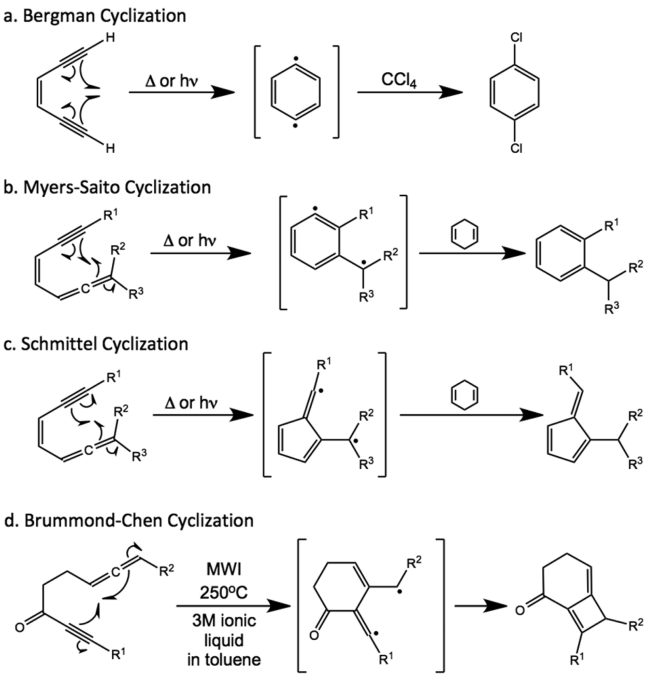

Scheme 2

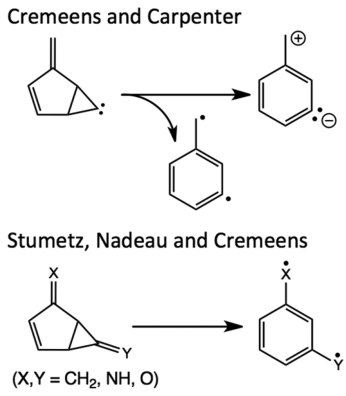

(Scheme 1c), and in some cases, formal (2 + 2) cycloadducts were also observed.[4] Many formal pericyclic reactions have also been shown to proceed via diradical intermediates, some of which reside on "calderas" or "mesas" on their potential energy surfaces (PESs) and involve so-called "twixtyls" and "continuous diradicals."[5] In 2005, Brummond and Chen described a way to form cross-conjugated dienones via the thermal intramolecular

Received: March 11, 2016
Published: May 26, 2016

DOI: 10.1021/acs.joc.6b00533
J. Org. Chem. 2016, 81, 5295–5302

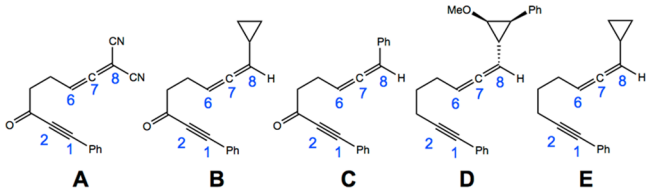

Figure 2. Allene-ynes examined herein.

(2 + 2)-cycloaddition of unconjugated allene-ynes,[6] a methodology later utilized in natural products total synthesis.[7] Our density functional studies indicated that these reactions proceed via allyl/vinyl diradicals (Scheme 1d).[8] We were intrigued, however, by the observation that some transition state structures leading to diradicals were closed-shell, and apparently zwitterionic in nature.[9] Herein we describe a detailed study on this issue, the results of which indicate the potential for an unusual

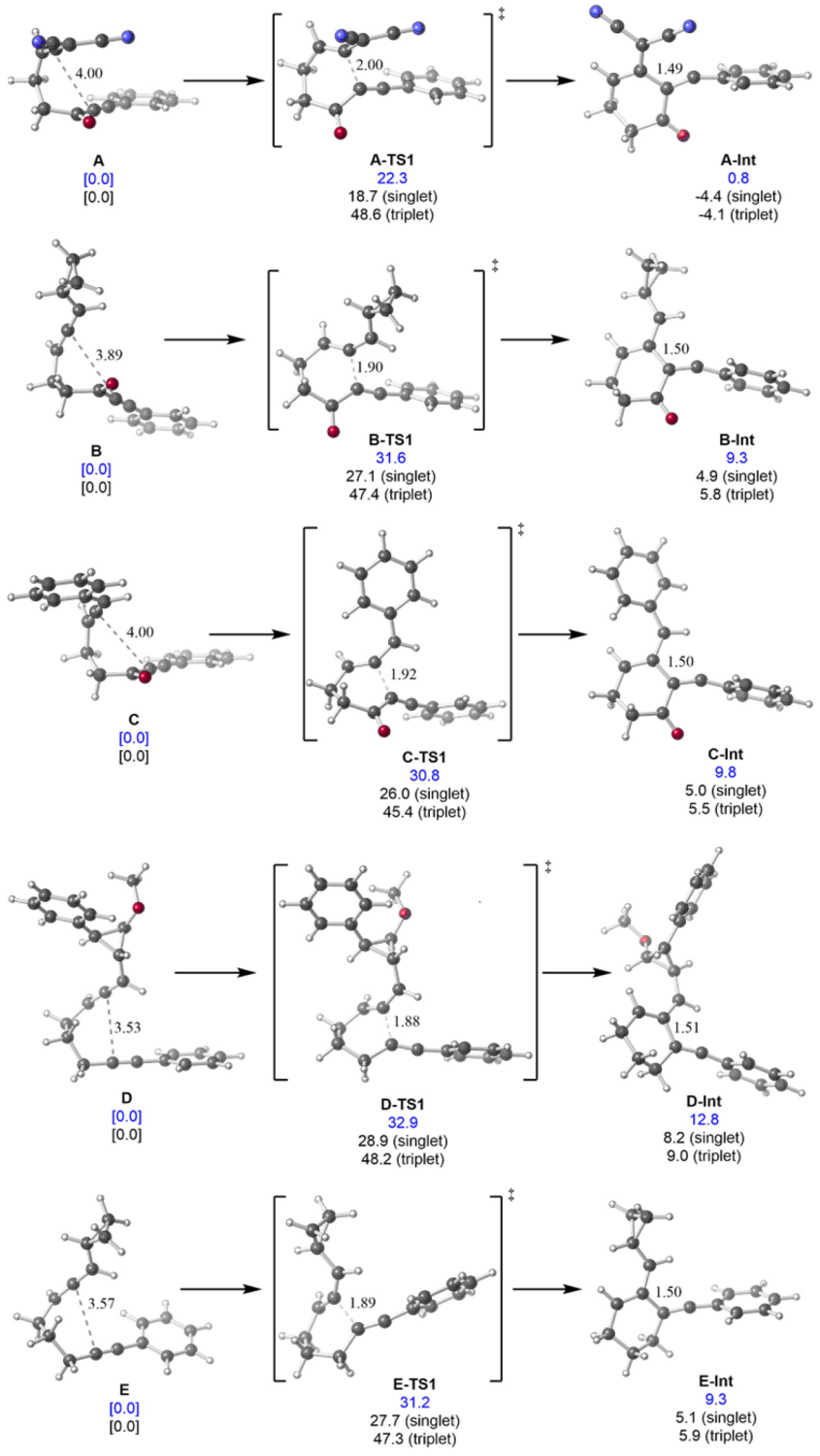

Figure 3. Transition state structures for C2−C7 bond formation. The blue numbers are relative Gibbs free energies for singlet structures (kcal/mol) with respect to the indicated [0.0]. The black numbers are relative electronic energies of the singlet and triplet structures (kcal/mol) with respect to the indicated [0.0]. Distances shown are in Å.

DOI: 10.1021/acs.joc.6b00533
J. Org. Chem. 2016, 81, 5295−5302

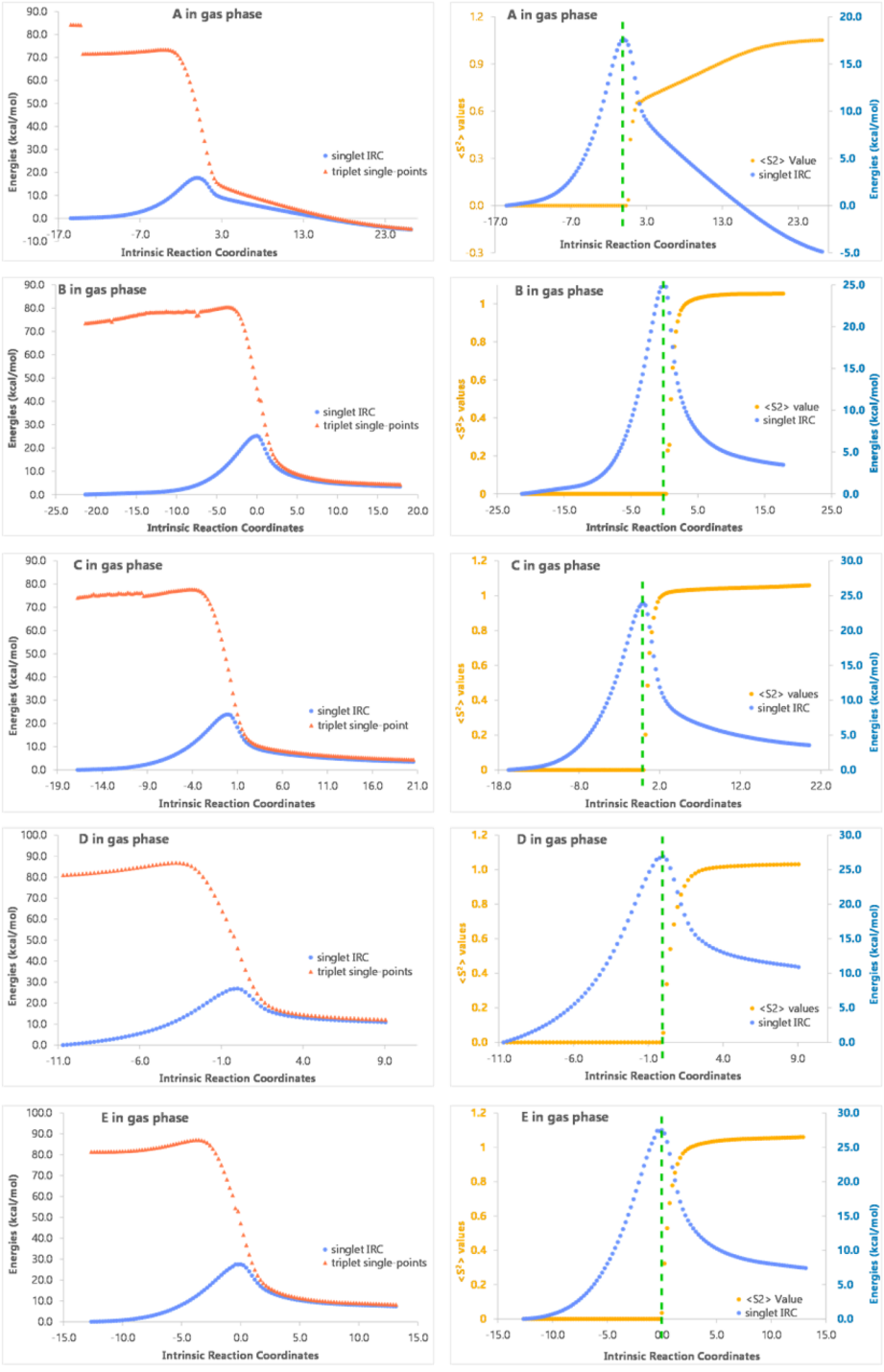

Figure 4. IRC plots for TSSs for systems **A**–**E**. Left: Singlet electronic energy vs reaction coordinate curves are shown in blue; triplet electronic energy vs reaction coordinate curves are shown in red-orange. Right: Singlet electronic energy vs reaction coordinate curves (expanded as compared to the lefthand plots) are shown in blue; the $\langle S^2 \rangle$ values vs reaction coordinate curves are shown in gold-orange; the vertical green dotted line indicates the location of the TSS points.

solvent-controlled switch between diradical and zwitterionic mechanisms.

Some previous work has explored the potential for accessing diradicals and zwitterions in the same reaction. In their 1992 article on the preparation and reactivity of (*Z*)-1,2,4-heptatrien-6-yne, Myers, Dragovich, and Kuo noted that apparent products of trapping both a phenyl/benzyl diradical (Scheme 1b) and a zwitterionic phenyl anion/benzyl cation (some describe these sorts of structures as "orbital isomers"[10]) can be formed, which one predominates depending on the solvents used.[3a] In 1999, on the basis of trapping experiments and computations (HF, MP2, CAS, DFT), Hughes and Carpenter suggested that this allene-ene-yne cyclization involved parallel biradical and polar (via a zwitterion or strained allene intermediate) mechanisms that branched from each other after the rate-determining transition state structure.[11] They also noted: "It is possible that a crossing to the open-shell electronic surface occurs after the transition state, and this serves as the branching point for the reaction" (Figure 1).

DOI: 10.1021/acs.joc.6b00533
J. Org. Chem. 2016, 81, 5295−5302

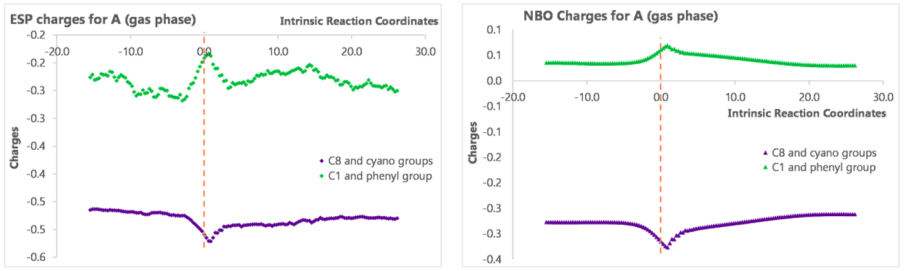

Figure 5. Charge vs reaction coordinate plots. Sum of the charges on C8 plus the attached substituents (purple) and sum of charges on C1 plus the attached phenyl group (green).The vertical dotted line indicates the position of the TSS.

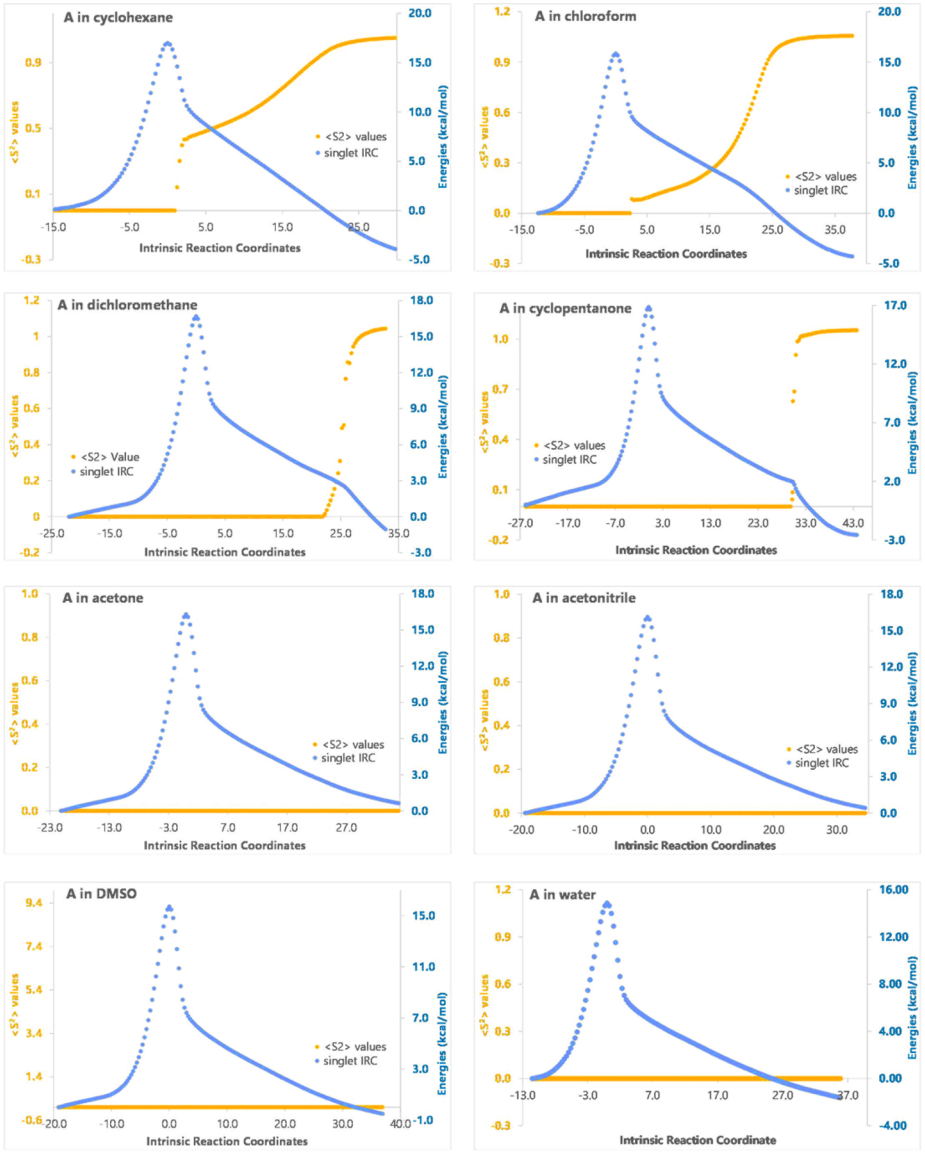

Figure 6. IRC plots for C2−C7 bond formation TSS for **A** in various solvents (here, using SMD). Singlet energy vs reaction coordinate plots are shown in blue. $\langle S^2 \rangle$ value vs reaction coordinate plots are shown in gold-orange.

In 2001, Cramer and co-workers used DFT calculations to predict that the product distribution of Myers-Saito vs Schmittel cyclization, as well as the preference for diradical vs closed-shell singlet intermediates, could be influenced by oxyanion substitution on the allene-ene-ynes.[12] In 2004, calculations (DFT and CASSCF) by Cremeens and Carpenter indicated that 4-methylene-bicyclo[3.1.0]hex-2-ene-6-ylidene can ring open under thermal conditions to produce the phenyl/benzyl diradical shown in Scheme 2 (top) via a post-transition state conical intersection;[13] in this case, the reaction was predicted to proceed toward the zwitterion after the transition state structure but then to follow the diradical surface after the conical intersection—a nonadiabatic process. In a follow-up to their 1999 study, Carpenter and co-workers concluded in 2005 that allene-ene-yne

DOI: 10.1021/acs.joc.6b00533
J. Org. Chem. 2016, 81, 5295−5302

cyclization also involves a post-transition state conical intersection that allows access to both zwitterion and the diradical intermediates.[14] In 2013, Stumetz, Nadeau, and Cremeens described calculations (CASSCF and DFT) on the ring-opening of 4,6-dimethylidenebicyclo[3.1.0]hex-2-ene derivatives to form bis-benzyl diradical intermediates (Scheme 2, bottom), predicting that post-transition state crossings between the singlet and triplet surfaces occur for these reactions.[15] Related "two-state reactivity" has been described for inorganic reactions involving transition metals.[16] We wondered whether similar post-transition state surface crossings were occurring in the Brummond–Chen cyclizations we had examined previously (Scheme 1d).[8,9]

METHODS

Using *Gaussian09*,[17] optimization and frequency calculations for minima and transition state structures (TSSs) were carried out without symmetry constraints using the unrestricted B3LYP/6-31+G(d,p)[18] method with the "guess = (mix,always)" designation (to allow for singlet diradical species). Despite its deficiencies, B3LYP appears to perform reasonably well for diradicals, as long as one accounts for spin contamination in singlets.[19] Frequency calculations were carried out at 250 °C. Intrinsic reaction coordinate (IRC) calculations[20] were performed on each TSS to locate connected minima as well as the lowest energy path that connects them to the TSSs. Single point energy calculations were also performed on IRC points and stationary points with an enforced triplet spin state using (U)B3LYP/6-31+G(d,p) (*vide infra*). This approach reproduced the results previously reported by Cremeens (ring-opening of 4,6-dimethylidenebicyclo[3.1.0]hex-2-ene derivative where X = O and Y=CH_2; see Supporting Information for details).[12] To further explore the validity of our results, CASSCF(8,8)/6-31G(d) calculations were performed for system **A** (Figure 2); see Supporting Information for details. Electrostatic potential-based (CHELPG, referred to as ESP later in the paper) and natural population analysis (NPA, also referred to as NBO) charges were also calculated for each IRC point of the singlet surface.[21] To investigate solvent effects, calculations were carried out using continuum models for cyclohexane, chloroform, dichloromethane, cyclopentanone, acetone, acetonitrile, and DMSO; the SMD,[22] CPCM,[23] and IEFPCM[24] methods were all used to get a sense of the dependence of results on the nature of the solvent model used (*vide infra*). Structure images were produced with the *CYLView* software package.[25] This study was restricted to "productive" conformations of reactants, i.e., those resulting from IRC calculations. A discussion of "spin projection," which did not change our conclusions, can be found in the Supporting Information.

RESULTS AND DISCUSSION

Several allene-yne cyclization transition state structures were found previously to have $\langle S^2 \rangle$ values of zero; i.e., no diradical character, but lead to diradical minima.[8,9] These systems (Figure 2) are reexamined here, with additional calculations aimed at characterizing the nature of the switch from closed-shell (zwitterionic) to open-shell (diradical) along reaction coordinates for cyclization. These particular systems were examined, due to their relevance to previous experiments.[8,9]

Gas Phase Reactions. TSSs for C2–C7 bond formation for each allene-yne are shown in Figure 3 (gas phase; the Brummond group's experiments were carried out in toluene in the presence of 3 equiv of an ionic liquid[8]). In systems with two different substituents attached to the allene (**B**–**E**), two different TSSs were located (only the lowest energy TSSs are shown in Figure 3; for others, see the Supporting Information). The predicted barriers for C2–C7 bond formation (see Figure 2 for atom numbering) were approximately the same, 31–33 kcal/mol, for **B**–**E**, whereas **A** had a lower barrier, 22 kcal/mol (likely due to the *gem*-dicyano substructure, a carbanion stabilizing group,

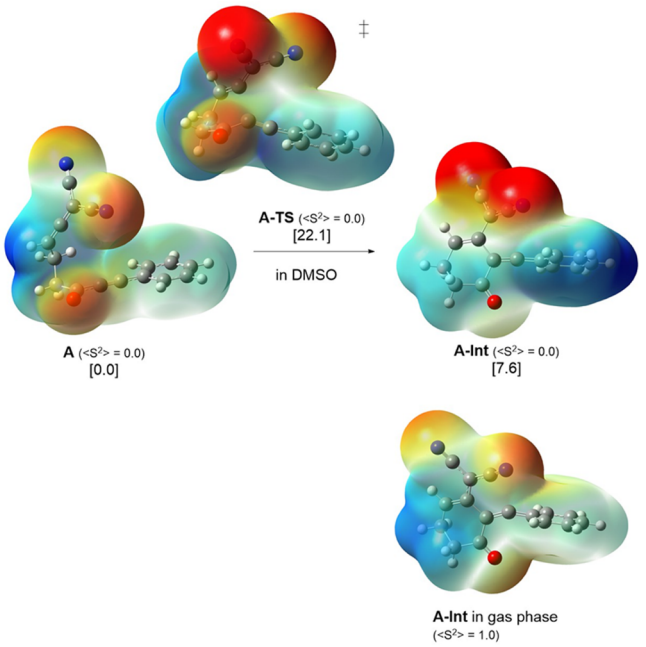

Figure 7. Electrostatic potential surfaces (isovalue = 0.0004 and charge range of −0.067 to 0.067) for stationary points involved in cyclization of **A** in DMSO (top; SMD), along with that for the intermediate optimized in the gas phase (bottom).

vide infra).[8,9] Single point energies for triplets with the geometries of the optimized singlet intermediates were also calculated and are shown in Figure 3. For all systems, the triplet energies were slightly above (by 0.3–0.9 kcal/mol) the singlet energies, with **A** having the smallest gap (0.3 kcal/mol). Thus, essentially no singlet–triplet gap was predicted for the intermediates formed upon C2–C7 bond formation, consistent with there being approximately no interaction between the distal radical centers. System **A** was also examined using CASSCF(8,8)/6-31G(d). Using this method, a barrier (electronic energies) of 20.0 kcal/mol was predicted for the singlet reaction (cf. 18.7 kcal/mol with UB3LYP) and a singlet–triplet gap of 1.7 kcal/mol (favoring the singlet; cf. 0.3 kcal/mol favoring the singlet with UB3LYP) was predicted, suggesting that the UB3LYP energetics are likely reasonable.

We also examined how the singlet/triplet gap changes along the IRC for each reaction. The graphs in the left column of Figure 4 show the singlet electronic energies of the points along the IRC (blue curve) for each reaction, along with the triplet energies of each point (red-orange curves), determined by running single point calculations on each singlet geometry. Note that our single points provide a single path/seam on the excited state surface that is not necessarily the lowest energy path (it is almost certainly not). In contrast to the reaction studied by Cremeens and co-workers,[12] our computed triplet pathways do not cross the corresponding singlet pathways, but rather merge as the intermediate is approached (see the Supporting Information for results of test calculations with CASSCF, the results of which support this picture of reactivity).

To characterize the onset of diradical character along the reaction coordinate for each bond forming reaction, we examined the $\langle S^2 \rangle$ values (see Supporting Information for data on atomic spin densities). Pure singlets (diradical or not) should have $\langle S^2 \rangle$ values of 0, while triplets have $\langle S^2 \rangle$ values of 2.0. Diradicals are often found to have $\langle S^2 \rangle$ values of approximately 1.0 in density functional theory (DFT) calculations; this value indicates an

DOI: 10.1021/acs.joc.6b00533
J. Org. Chem. 2016, 81, 5295–5302

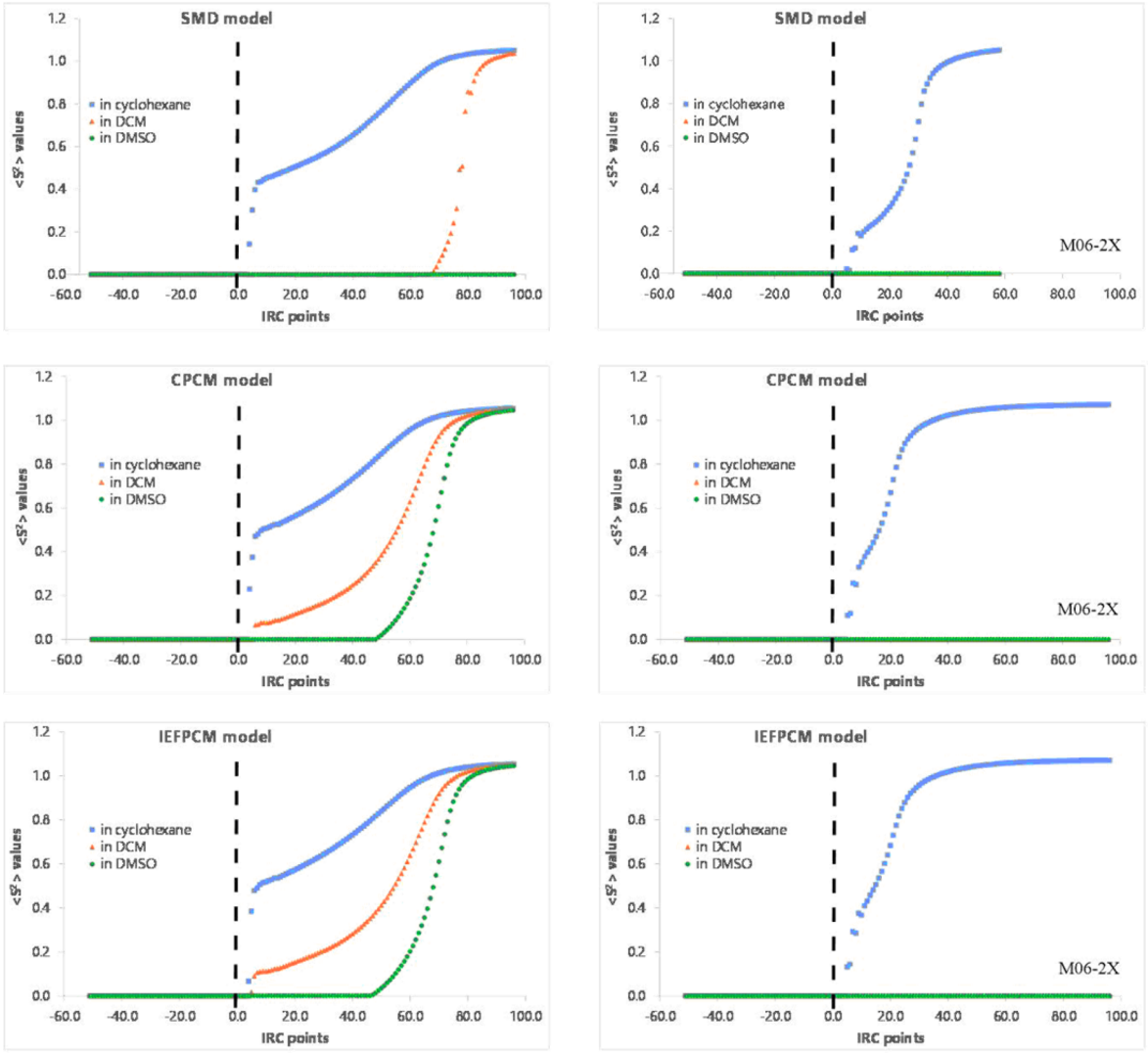

Figure 8. $\langle S^2 \rangle$ value vs IRC points for the reaction of **A** in cyclohexane (blue), dichloromethane (red-orange), and DMSO (green). The vertical dotted line indicates the position of the TSS. The left column corresponds to calculations done with UB3LYP/6-31+G(d,p), whereas the right column shows UM06-2X/6-31+G(d,p) results (note that, for the right-hand column, the orange line is coincident with the green line in all cases.).

equal mixture of singlet and triplet. Although $\langle S^2 \rangle$ values of approximately 1.0 can be viewed, as indicating severe contamination of a ground state by a higher energy triplet state, this value can also be taken as a marker of diradicals that lack communication between their two radical centers.[16] $\langle S^2 \rangle$ values for the TSSs for cyclization of **A**, **B**, and **C** were 0.0, while those for TSSs for cyclization of **D** and **E** were 0.05 and 0.03, respectively, indicating very little to no diradical character at any of the TSSs.[26] All intermediates were found to have $\langle S^2 \rangle$ values of approximately 1.0, as expected for diradical structures. The right-hand plots in Figure 4 show $\langle S^2 \rangle$ values (gold-orange) for each point along each IRC.[27] For all systems, $\langle S^2 \rangle$ values increased above zero at or just after the TSS (for **D** and **E**, the $\langle S^2 \rangle$ value increased above zero at the TSS; for **C**, the $\langle S^2 \rangle$ value increased above zero at the IRC point immediately following the TSS; for **B**, the $\langle S^2 \rangle$ value increased above zero two IRC points after the TSS; for **A**, the $\langle S^2 \rangle$ value increased above zero five IRC points after the TSS). Note that the slight differences in the position of onset of diradical character track with the computed singlet−triplet gaps of the intermediates. Note also that the TSS for **A** also has the longest C2−C7 distance. System **A** is the most interesting, as structures in the immediate vicinity of the TSS had no diradical character, suggesting that this TSS is closed shell (perhaps zwitterionic; *vide infra*) in nature, despite the fact that it leads to a diradical intermediate. Having a zwitterionic TSS in a (di)radical-forming reaction opens up avenues for rate modulation not usually associated with radical-forming processes.[28]

To characterize the onset of zwitterionic character along the reaction coordinate for each bond forming reaction, we examined charges for each point of each IRC.[17] Plots for **A** are shown in Figure 5. The sum of the charges on C8 plus the attached substituents is shown in purple, and the sum of the charges on C1 plus the attached phenyl group is shown in green, for each point. With both CHELPG and NPA charge models, there is a small but clear separation of charge as the TSS is reached, which increases until diradical character appears, at which point it decreases. This behavior is consistent with a reaction proceeding toward a zwitterion that, before full expression of zwitterionic character, "changes direction" and forms a diradical intermediate. Behavior for the other systems, with less electron-withdrawing substituents on C8, was more difficult to rationalize (see Supporting Information).

Solvent Effects. In light of the above results, we questioned whether the onset of diradical character could be delayed by

DOI: 10.1021/acs.joc.6b00533
J. Org. Chem. 2016, 81, 5295−5302

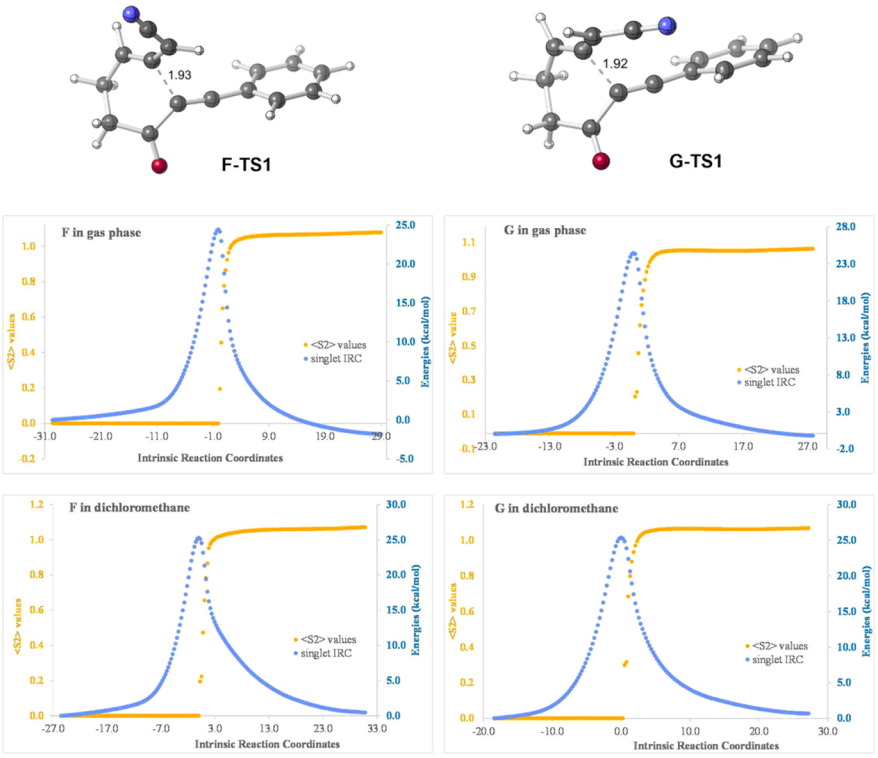

Figure 9. IRC plots (UB3LYP) for the C2−C7 bond formation TSS for **F** and **G** in gas phase and DCM (using SMD). Singlet energy vs reaction coordinate plots are shown in blue. $\langle S^2 \rangle$ value vs reaction coordinate plots are shown in gold-orange.

increasing the polarity of the environment, which would favor zwitterionic species. We recomputed the TSS for C2−C7 bond formation of **A** in cyclohexane (ε = 2.02), chloroform (ε = 4.71), dichloromethane (ε = 8.93), cyclopentanone (ε = 13.58), acetone (ε = 20.49), acetonitrile (ε = 35.69), DMSO (ε = 46.83), and water (ε = 78.35), first using the SMD continuum approach (see the Methods section). As expected, the onset of diradical character, as measured by computed $\langle S^2 \rangle$ values, moved later along the IRC as solvent dielectric constant increased (Figure 6; the $\langle S^2 \rangle$ value became greater than zero at the fourth point after the TSS in the gas phase (see Figure 4), at the third point after the TSS in cyclohexane, at the seventh point after the TSS in chloroform, at the 67th point after the TSS in dichloromethane, and at the 91st point after the TSS in cyclopentanone). With acetone, acetonitrile, DMSO, and water the $\langle S^2 \rangle$ value remained zero along the entire IRC, suggesting that, in environments of high enough polarity, a diradical intermediate might be avoided completely.[29] Consistent with this conjecture, the intermediate for system A was found to have an $\langle S^2 \rangle$ value of approximately 1.0 when fully optimized in cyclohexane, chloroform, dichloromethane, cyclopentanone, and acetone, but a value of 0.0 with acetonitrile, DMSO, and water. Electrostatic potential surfaces (Figure 7) show clearly that charge separation increases along the reaction coordinate in DMSO and that the intermediate has considerably less charge separation in the gas phase. We also reexamined the corresponding reactions for **B**−**E** in DMSO, but solvent had little to no apparent effect for these systems (see Supporting Information).

To probe whether the diradical/zwitterion switch was dependent on the solvent model and/or functional used, we reran TSS and IRC calculations for **A** in cyclohexane, dichloromethane, and DMSO with different solvent models—CPCM and IEFPCM—and with the M06-2X functional (also unrestricted calculations). First, consider the UB3LYP results (Figure 8, left-hand column). Although results obtained with CPCM and IEFPCM do not indicate that the $\langle S^2 \rangle$ value will remain zero throughout the entire IRC in DMSO, the three solvent models agree with respect to the overall trend: as the dielectric constant of the solvent increases, the $\langle S^2 \rangle$ value remains 0.0 further along the IRC. Next, consider the UM06-2X results (Figure 8, right-hand column). With this functional, both DCM and DMSO are predicted to be polar enough to suppress diradical formation, no matter which solvent model is used. Given the observed variation in results, we cannot make a firm prediction as to whether or not a zwitterionic intermediate would actually form in a particular solvent, but the possibility that it would is intriguing.[30]

Substituent Effect. As described above, only **A**, the system with the most polarizing substituents, displayed significant solvent sensitivity. We therefore decided to examine a variant of **A** with one less nitrile substituent (Figure 9, top, shows TSSs for two geometric isomers, **F** and **G**) to see if the solvent sensitivity would persist. While **A** maintained an $\langle S^2 \rangle$ value of 0.0 for >60 post-TSS IRC points in DCM, **F** and **G** showed no significant deviations from gas phase behavior. Clearly, an extremely electron-deficient C8 is required for a meaningful solvent effect (at least in the absence of explicit intermolecular interactions).

CONCLUSIONS

Intrigued by the possibility of accessing diradical intermediates from zwitterionic transition state structures, we reexamined several Brummond−Chen (2 + 2) cycloaddition reactions.[6,8,9] Our computational results indicate that singlet and triplet surfaces likely do not cross, but rather converge as intermediates are formed. For one system with substituents predisposed to selectively stabilize polar structures (**A**), significant charge separation (zwitterionic character) was predicted for the cyclization TSS. In addition, it was shown that the onset of diradical character

DOI: 10.1021/acs.joc.6b00533
J. Org. Chem. 2016, 81, 5295−5302

can be delayed by increasing solvent polarity, perhaps even to the point where diradical formation is suppressed completely.

■ ASSOCIATED CONTENT

Supporting Information

The Supporting Information is available free of charge on the ACS Publications website at DOI: 10.1021/acs.joc.6b00533.

Details on computational methods and additional results mentioned in the text (PDF)

Atomic coordinates for computed structures (MOL)

■ AUTHOR INFORMATION

Corresponding Author

*E-mail: djtantillo@ucdavis.edu.

Notes

The authors declare no competing financial interest.

■ ACKNOWLEDGMENTS

We are grateful to the National Science Foundation (XSEDE program, CHE030089) for computer support, Kay Brummond for introducing us to this fascinating reaction, Matthew Siebert for carrying out the initial calculations that inspired this project, and Ryan Pemberton for advice.

■ REFERENCES

(1) Bergman, R. G. *Acc. Chem. Res.* **1973**, *6*, 25−31.

(2) (a) Myers, A. G. *Tetrahedron Lett.* **1987**, *28*, 4493−4496. (b) Saito, K.; Watanabe, T.; Takahashi, K. *Chem. Lett.* **1989**, 2099−2102.

(3) (a) Myers, A. G.; Dragovich, P. S.; Kuo, E. Y. *J. Am. Chem. Soc.* **1992**, *114*, 9369−9386. (b) Myers, A. G.; Kuo, E. Y.; Finney, N. S. *J. Am. Chem. Soc.* **1989**, *111*, 8057−8059. (c) Nagata, R.; Yamanaka, H.; Murahashi, E.; Saito, I. *Tetrahedron Lett.* **1990**, *31*, 2907−2910. (d) Grissom, J. W.; Gunawardena, G. U.; Klingberg, D.; Huang, D. *Tetrahedron* **1996**, *52*, 6453−6518. (e) Schreiner, P. R.; Prall, M. *J. Am. Chem. Soc.* **1999**, *121*, 8615−8627.

(4) Schmittel, M.; Strittmatter, M.; Kiau, S. *Tetrahedron Lett.* **1995**, *36*, 4975−4978.

(5) Examples and leading references: (a) Gutierrez, O.; Harrison, J. G.; Pemberton, R. P.; Tantillo, D. J. *Chem. - Eur. J.* **2012**, *18*, 11029−11035. (b) Leach, A. G.; Catak, S.; Houk, K. N. *Chem. - Eur. J.* **2002**, *8*, 1290−1299. (c) Baldwin, J. E.; Leber, P. A. *Org. Biomol. Chem.* **2008**, *6*, 36−47. (d) Doering, W. v. E.; Eklmanis, J. L.; Belfield, K. D.; Klarner, F. G.; Krawzyk, B. *J. Am. Chem. Soc.* **2001**, *123*, 5532−5541. (e) Doering, W. v. E.; Sachdev, K. *J. Am. Chem. Soc.* **1974**, *96*, 1168−1187. (f) Carpenter, B. K. *Chem. Rev.* **2013**, *113*, 7265−77286. (g) Hoffmann, R.; Swaminathan, S.; Odell, B. G.; Gleiter, R. *J. Am. Chem. Soc.* **1970**, *92*, 7091−7097.

(6) Brummond, K. M.; Chen, D. *Org. Lett.* **2005**, *7*, 3473−3475.

(7) Ovaska, T. V.; Kyne, R. E. *Tetrahedron Lett.* **2008**, *49*, 376−378.

(8) Siebert, M. R.; Osbourn, J. M.; Brummond, K. M.; Tantillo, D. J. *J. Am. Chem. Soc.* **2010**, *132*, 11952−11966.

(9) Siebert, M. R. Ph.D. dissertation, University of California—Davis, 2005.

(10) Gonçalves, T. P.; Mohamed, M.; Whitby, R. J.; Sneddon, H. F.; Harrowven, D. C. *Angew. Chem., Int. Ed.* **2015**, *54*, 4531−4534.

(11) Hughes, T. S.; Carpenter, B. K. *J. Chem. Soc., Perkin Trans. 2* **1999**, 2291−2298.

(12) Cramer, C. J.; Kormos, B. L.; Seierstad, M.; Sherer, E. C.; Winget, P. *Org. Lett.* **2001**, *3*, 1881−1884.

(13) Cremeens, M. E.; Carpenter, B. K. *Org. Lett.* **2004**, *6* (14), 2349−2352.

(14) Cremeens, M. E.; Hughes, T. S.; Carpenter, B. K. *J. Am. Chem. Soc.* **2005**, *127*, 6652−6661.

(15) Stumetz, K. S.; Nadeau, J. T.; Cremeens, M. E. *J. Org. Chem.* **2013**, *78*, 10878−10884.

(16) Yoshizawa, K.; Shiota, Y.; Yamabe, T. *J. Chem. Phys.* **1999**, *111* (2), 538−545.

(17) *Gaussian 09*, Revision B.01; Gaussian, Inc.: Wallingford, CT, 2009 (full reference in Supporting Information).

(18) (a) Becke, A. D. *J. Chem. Phys.* **1993**, *98*, 5648−5652. (b) Lee, C.; Yang, W.; Parr, R. G. *Phys. Rev. B: Condens. Matter Mater. Phys.* **1988**, *37*, 785−789. (c) Miehlich, B.; Savin, A.; Stoll, H.; Preuss, H. *Chem. Phys. Lett.* **1989**, *157*, 200−206.

(19) Bally, T.; Borden, W. T. Calculations on Open-Shell Molecules: A Beginner' Guide. In *Reviews in Computational Chemistry*; Lipkowitz, K. B., Boyd, D. B., Eds.; John Wiley & Sons, Inc.: Hoboken, NJ, 1999; Vol. 3, pp 1−97.

(20) (a) Fukui, K. *Acc. Chem. Res.* **1981**, *14*, 363−368. (b) Gonzalez, C.; Schlegel, H. B. *J. Phys. Chem.* **1990**, *94*, 5523−5527. (c) Maeda, S.; Harabuchi, Y.; Ono, Y.; Taketsugu, T.; Morokuma, K. *Int. J. Quantum Chem.* **2015**, *115*, 258−269.

(21) CHELPG: Breneman, C. M.; Wiberg, K. B. *J. Comput. Chem.* **1990**, *11*, 361−371. NBO: (a) Foster, J. P.; Weinhold, F. *J. Am. Chem. Soc.* **1980**, *102*, 7211−7218. (b) Reed, A. E.; Weinhold, F. *J. Chem. Phys.* **1983**, *78*, 4066−4073. (c) Reed, A. E.; Weinstock, R. B.; Weinhold, F. *J. Chem. Phys.* **1985**, *83*, 735−746. (d) Reed, A. E.; Weinhold, F. *J. Chem. Phys.* **1985**, *83*, 1736−1740. (e) Carpenter, J. E. Ph.D. thesis, University of Wisconsin, Madison, WI, 1987. (f) Carpenter, J. E.; Weinhold, F. *J. Mol. Struct.: THEOCHEM* **1988**, *169*, 41−62. (g) Reed, A. E.; Curtiss, L. A.; Weinhold, F. *Chem. Rev.* **1988**, *88*, 899−926. Weinhold, F.; Carpenter, J. E. In *The Structure of Small Molecules and Ions*; Naaman, R., Vager, Z., Eds.; Plenum: 1988; pp 227−236.

(22) Marenich, A. V.; Cramer, C. J.; Truhlar, D. G. *J. Phys. Chem. B* **2009**, *113*, 6378−6396.

(23) (a) Barone, V.; Cossi, M. *J. Phys. Chem. A* **1998**, *102*, 1995−2001. (b) Cossi, M.; Rega, N.; Scalmani, G.; Barone, V. *J. Comput. Chem.* **2003**, *24*, 669−681.

(24) Scalmani, G.; Frisch, M. J. *J. Chem. Phys.* **2010**, *132*, 114110.

(25) Legault, C. Y. *CYLview*, 1.0b; Université de Sherbrooke: 2009; (http://www.cylview.org).

(26) Borden and co-workers found $\langle S^2 \rangle$ values of 0.3 for TSSs in other diradical-forming reactions. See: Hrovat, D. A.; Duncan, J. A.; Borden, W. T. *J. Am. Chem. Soc.* **1999**, *121*, 169−175.

(27) Similar plots have been constructed for other reactions, e.g., see: *Chem. Phys. Lett.* **1993**, *216*, 380−388.10.1016/0009-2614(93)90113-F

(28) (a) Litwinienko, G.; Beckwith, A. L. J.; Ingold, K. U. *Chem. Soc. Rev.* **2011**, *40*, 2157−2163. (b) Possible effects due to hydrogen-bonding: Guha, A. K.; Boruah, A.; Hazarika, M.; Kaman, S. *Rep. Theor. Chem.* 2015, *3*, 1−6 and references therein.. (c) Alabugin and co-workers have reviewed the panopoly of organic reactions in which bonds are broken to form diradical or zwitterion intermediates (the so-called "diradical/zwitterion dichotomy"); see: Peterson, P. W.; Mohamed, R. K.; Alabugin, I. V. *Eur. J. Org. Chem.* **2013**, *2013*, 2505−2527. and Mohamed, R. K.; Peterson, P. W.; Alabugin, I. V. *Chem. Rev.* **2013**, *113*, 7089−7129.

(29) Note that the onset of nonzero $\langle S^2 \rangle$ values appears to correlate with changes to the slope of the IRC curves.

(30) See the Supporting Information for a summary of $\langle S^2 \rangle$ values and relative energies for stationary points.

DOI: 10.1021/acs.joc.6b00533
J. Org. Chem. 2016, 81, 5295−5302